

## Diluted magnetic $\text{Ce}_{1-2x}\text{Co}_x\text{Zn}_x\text{O}_{2-\delta}$

T.S. Santos, A.N. Rodrigues and M.A. Macêdo  
*Department of Physics, Federal University of Sergipe,*  
*49000-100, São Cristóvão, SE, Brazil,*  
*e-mail: mmacedo@ufs.br*

Recibido el 25 de junio de 2010; aceptado el 23 de abril de 2011

$\text{Ce}_{1-2x}\text{Zn}_x\text{Co}_x\text{O}_{2-\delta}$  powders obtained from the proteic sol-gel process were studied by magnetic measurements. Magnetization measurements indicate that Co doping can induce at room temperature ferromagnetism, perhaps induced by oxygen vacancies. From X-ray diffraction analysis no secondary phase was observed in  $\text{Ce}_{1-2x}\text{Zn}_x\text{Co}_x\text{O}_{2-\delta}$  for  $x \leq 0.05$ .

*Keywords:*  $\text{CeO}_2$ ; proteic sol-gel; diluted magnetic semiconductors; ferromagnetism.

Polvos de  $\text{Ce}_{1-2x}\text{Zn}_x\text{Co}_x\text{O}_{2-\delta}$  obtenidos por el proceso sol-gel proteico fueron estudiados por medidas magnéticas. Mediciones de magnetización para indican que el dopaje de Co puede inducir ferromagnetismo a temperatura ambiente, tal vez inducido por vacantes de oxígeno. Del análisis de difracción de rayos X ninguna fase secundaria fue observada en  $\text{Ce}_{1-2x}\text{Zn}_x\text{Co}_x\text{O}_{2-\delta}$  para  $x \leq 0.05$ .

*Descriptores:*  $\text{CeO}_2$ ; proteic sol-gel; semiconductores magnéticos diluidos; ferromagnetismo.

PACS: 61.05.cp; 75.50.Pp; 78.40.Fy

### 1. Introduction

Semiconductors that exhibit ferromagnetism at room temperature (RTFM) have attracted the interest of the scientific community because they are the key to the achievement of future spintronic devices. Spintronics is the manipulation of degrees of freedom of spin and charge carriers [1], aiming at producing devices that have faster processors, lower power consumption, storage in a single chip etc. In order to achieve these goals it is necessary an efficient injection of spin, slow spin relaxation, and reliable detection of spin. Diluted magnetic semiconductors (DMS) are a promising class of materials to achieve these goals [2,3]. The first attempts to achieve the DMS have been with II-VI semiconductors although it is difficult to control the doping process in these materials. This is the biggest obstacle to its use as spintronic materials. Another class of interesting materials is that of the semiconductors of type III-V in which GaAs is the most known material. Much of the success of (Ga,Mn)As DMS comes from the substitution of trivalent Ga for Mn, where Mn becomes simultaneously the source of magnetic moment and acceptor level, but when Mn occupies an interstitial position it becomes a double donor and does not contribute to the ferromagnetism mediated by carriers, which is a problem [4-6]. Alternatively, good performances with respect to magnetic and semiconductor properties have been found for several oxides (ZnO,  $\text{Cu}_2\text{O}$ ,  $\text{SnO}_2$  and  $\text{CeO}_2$ ) can support deviations in stoichiometry of  $\text{CeO}_{2-\delta}$  with  $0 < \delta < 0.5$ ) doped with transition metals [7-9].

The origin of the RTFM in semiconductor oxides is different from the established origin for magnetism in oxides, where moments are located the 3d, 4d or 4f shells and the coupling is a nearest-neighbour superexchange or double exchange interaction [10]. Some works report that these conventional interactions are incapable of explaining the long-

range magnetic order when the concentrations of magnetic cations are below the percolating threshold and the ferromagnetic exchange is mediated through electron donors of more external layers. That is, the origin of this confined behavior must be a magnetic percolation of polarons, which could be correlated to the presence of oxygen vacancies and defects in the lattice of the material [10,11]. The goal of the present research was to prepare samples of Zn-Co-doped  $\text{CeO}_2$  by the proteic sol-gel process, as well as to study the influence of the Zn and Co ions on magnetic and structural properties of this material.

### 2. Experimental

A proteic sol was prepared by dissolving hexahydrated zinc nitrate ( $\text{Zn}(\text{NO}_3)_2 \cdot 6\text{H}_2\text{O}$ ), hexahydrated cobalt nitrate ( $\text{Co}(\text{NO}_3)_2 \cdot 6\text{H}_2\text{O}$ ) and ammonium cerium (IV) nitrate ( $(\text{NH}_4)_2\text{Ce}(\text{NO}_3)_6$ ) in filtered coconut water (*Cocos nucifera*) with  $x = 0.01, 0.05$  and  $0.1$  to obtain the  $\text{Ce}_{1-2x}\text{Zn}_x\text{Co}_x\text{O}_{2-\delta}$ . Afterwards, the sol was heated at  $100^\circ\text{C}$  for 24 h for gelification-dehydration and then at  $400^\circ\text{C}$  for 1 h for decomposition of the salts. Finally, it was calcinated at  $600$  and  $800^\circ\text{C}$  for 1 h in air to eliminate the organic materials and to completely oxidize the salts [9]. Crystalline phases were identified by X-ray diffraction (DRX) measurements using  $\text{CuK}\alpha$  radiation at 40 kV/ 40 mA with the Rigaku RINT 2000/PC diffractometer in the Bragg-Bretano geometry in the  $2\theta$  range in the  $25-75^\circ$ , in steps of  $0.02^\circ$ , and with a counting time of 5 s per step. The pattern was electronically identified using the JCPDS database. Raman spectroscopy was performed between 200 and  $1400\text{ cm}^{-1}$  using a SENTERRA Dispersive Raman Microscope with a laser of 633 nm. Magnetization was measured using a Quantum Design MPMS5 magnetometer with a maximum field of  $\pm 70\text{ kOe}$ .

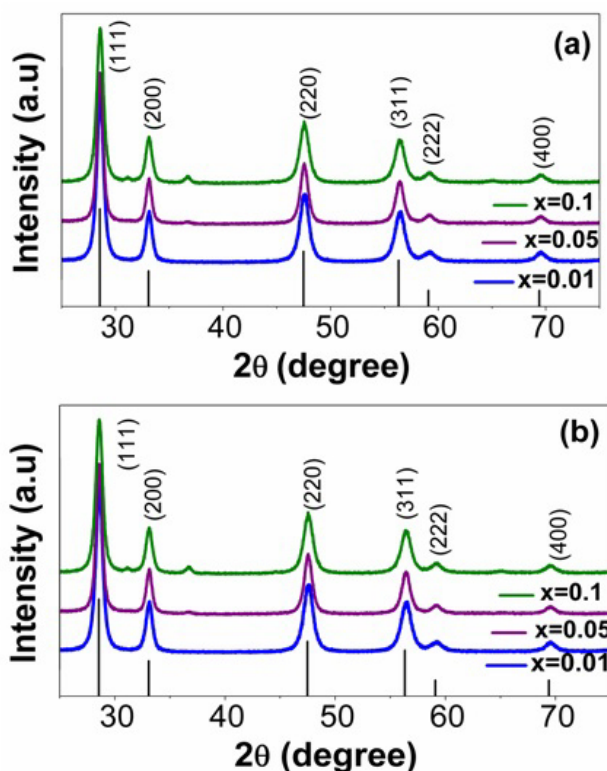


FIGURE 1. XRD patterns recorded at room temperature for samples  $Ce_{1-2x}Zn_xCo_xO_{2-\delta}$  prepared at (a) 600°C and (b) 800°C with varying dopant concentrations. The expected peak positions are indicated for  $CeO_2$  along the x-axis.

### 3. Results and discussion

Figure 1 shows the XRD patterns for  $Ce_{1-2x}Zn_xCo_xO_{2-\delta}$  powders with  $x = 0.01, 0.05$  and  $0.1$  that correspond to 1, 5 and 10%, respectively. The peak positions matched the powder diffraction data for  $CeO_2$  obtained by using JCPDS #34-0394 (vertical lines below the patterns), which suggests a cubic symmetry belonging to the Fm-3m space group. Spurious phases of the cobalt oxide ( $2\theta=37^\circ$ ) and zinc oxide ( $2\theta=31^\circ$ ) were observed for samples with  $x = 0.1$  calcinated at 600°C and 800°C and with  $x = 0.05$  calcinated at 600°C, indicating that the maximum doping is between 5 and 10%. The doping limit is extremely low because there is a competition between  $Zn^{2+}$  and  $Co^{2+}$  ions that replaces the  $Ce^{4+}$  ions. There is a possible mechanism of doping  $Zn^{2+}$  or  $Co^{2+}$  substituting any one of them by  $Ce^{4+}$  ions, creating thus oxygen vacancies ( $O^{2-}$ ) for charge balancing [12]. The peak width decreased with increase in calcination temperature, indicating a better crystallization of the samples. We observed the decrease of the spurious peaks for sample calcinated at 800°C with the formation of a single phase of the  $CeO_2$  for  $x \leq 0.05$ .

Figure 2 shows the Raman spectra for  $Ce_{1-2x}Zn_xCo_xO_{2-\delta}$  powders with  $x = 0.01, 0.05$  and  $0.1$ .  $CeO_2$  with a fluorite structure has only one vibrational Raman mode, which is a symmetrical mode of expansion and contraction of oxygen atoms around each cation, with Raman vibrational frequency

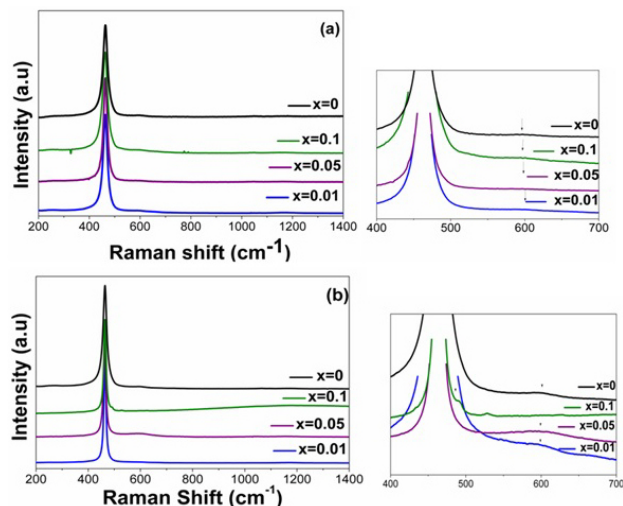


FIGURE 2. Raman spectra of  $Ce_{1-2x}Zn_xCo_xO_{2-\delta}$  with variation of  $x = 0, 0.01, 0.05$  and  $0.1$  for samples calcinated at (a) 600 and (b) 800°C.

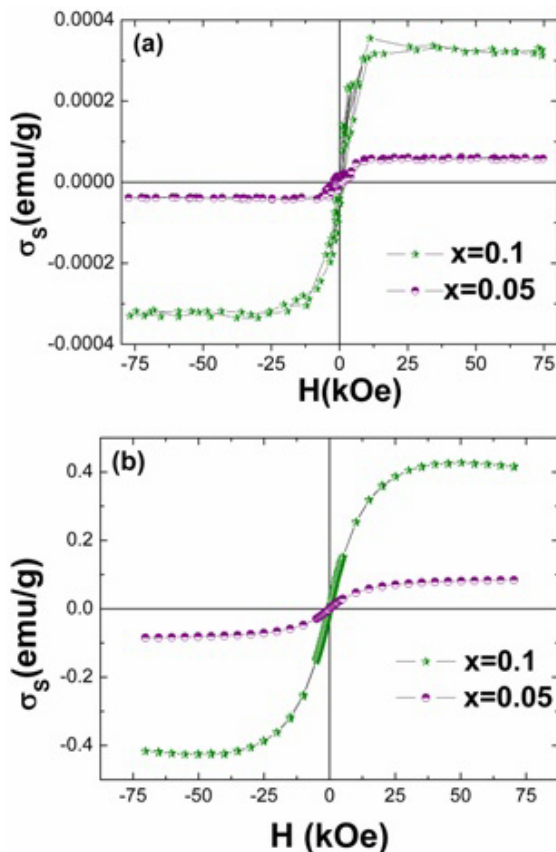


FIGURE 3. Magnetization loop at (a) 2 and (b) 300 K for  $Ce_{1-2x}Zn_xCo_xO_{2-\delta}$  with variation of  $x = 0.1$  and  $0.05$  for samples calcinated at 800°C.

around  $468\text{ cm}^{-1}$ , which is attributed to the vibrational mode of the Ce-O8 and the oxygen vacancy vibrational mode was measured in  $595\text{ cm}^{-1}$ [9]. Spurious phases of the  $Co_3O_4$  were observed in wavenumbers 500 and  $530\text{ cm}^{-1}$  in the

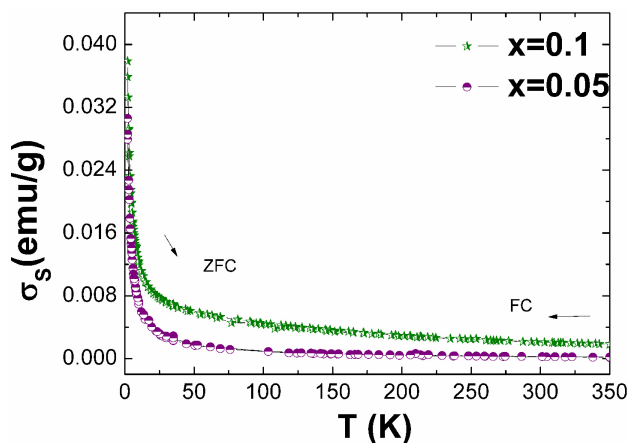


FIGURE 4. Magnetization versus temperature (ZFC and FC) for  $Ce_{1-2x}Zn_xCo_xO_{2-\delta}$  with variation of  $x = 0.1$  and  $0.05$  for samples calcined at  $800^\circ C$ .

doped samples with 10% of Co and calcinated at  $800^\circ C$ , confirming the results of XRD. Raman spectroscopy shows the behavior surface of the particles, so the  $CeO_2$  involves the spurious phases of the Zn and Co oxides.

The magnetization versus magnetic field and magnetization versus temperature were carried on for the samples with  $x = 0.1$  and  $0.05$  and calcination temperature of  $800^\circ C$ . Figure 3 shows the curves of magnetization versus field of the samples of  $Ce_{1-2x}Zn_xCo_xO_{2-\delta}$  powders with  $x=0.1$  and  $0.05$ . They present a magnetization of saturation ( $M_S$ ) which increases with zinc and cobalt concentrations. The samples showed ferromagnetism at room temperature ( $300 K$ ), where  $M_S$  was  $0.0004$  emu/g for the sample with  $x = 0.1$  and  $0.0001$  emu/g for the sample with  $x = 0.05$ .

The magnetization of saturation at  $2 K$  for the doping of 10% was  $0.4$  emu/g, and for the doping of 5% the magnetization of saturation was  $0.1$  emu/g. The small values of the remanent magnetization ( $M_r$ ) and coercive field ( $H_c$ ) for both temperatures ( $2$  and  $300 K$ ), indicate a trend of a super-

paramagnetic behavior. Moreover, the superparamagnetism can only be confirmed when  $M_r = H_c = 0$ . So we can infer that the samples showed a weak ferromagnetic behavior with high dilution of doping ions. The paramagnetic contribution was subtracted from the magnetization versus magnetic field curves.

Figure 4 shows the temperature dependence of the field-cooling and zero-field-cooling (FC and ZFC) with a magnetic field applied of  $1000 Oe$  for  $Ce_{1-2x}Zn_xCo_xO_{2-\delta}$  with variation of  $x = 0.1$  and  $0.05$  for samples calcinated at  $800^\circ C$ . The graphs show a large slope (temperature below  $50 K$ ) due to a paramagnetic contribution, indicating the existence of some ions without magnetic interactions in the matrix. The strong paramagnetic contribution led to the same behavior between the curves of ZFC and FC, preventing the saturation curve at low temperature for FC.

## 4. Conclusions

The ferromagnetic behavior can be attributed to the presence of magnetic ions mediated by  $O^{2-}$  vacancies. Spurious phases in the sample for  $x = 0.1$  can be eliminated by raising the calcination temperature. It is known that ZnO has a ferromagnetic behavior at room temperature also induced by oxygen vacancies. A study to be done in the future is the preparation of a mixed oxide  $CeO_2$ -ZnO to allow the insertion of ions in two crystalline matrices, ie, the structure wurtzita of the ZnO and fluorite type of the  $CeO_2$ .

## Acknowledgements

Tâmara S. Santos and Aline N. Rodrigues would like to acknowledge support from CAPES and CNPq, respectively, and the professor Mário Everaldo de Souza for reviewing this manuscript.

1. I. Zutic, J. Fabian, and S. Das Sarma, *Rev. Mod. Phys.* **76** (2004) 323-410.
2. H. Ohno and F. Matsukura, *Sol. St. Comm.* **117** (2001) 179.
3. T. Jungwirth *et al.*, *Rev. Mod. Phys.* **78** (2006) 809.
4. H. Ohno, *Science* **281** (1998) 951.
5. MacDonald *et al.*, *Nature Materials* **4** 195 (1998).
6. I. Kuryliszyn-Kudelska, *et al.*, *J. Appl. Phys.* **95** (2004) 603.
7. U. Ozgür, Y.I. Alivov, C. Liu, A. Teke, M.A. Reshchikov, S. Dogan, V. Avrutin, S.J. Cho, and H. Morkoc, *J. Appl. Phys.* **98** (2005) 041301.
8. S.J. Pearton, C.R. Abernathy, D.P. Norton, A.F. Hebard, Y.D. Park, L.A. Boatner, and J.D. Budai, *Mater. Sci. Eng. R* **40** (2003) 137.
9. P. Brito, D. Andrade, J.G.S. Duque, and M.A. Macêdo, *Physica B* **405** (2010) 1821.
10. J.M.D. Coey, *Curr. Opin. Solid State Mater. Sci.* **10** (2006) 83.
11. A. Kaminski, S.D. Sarma, *Phys. Rev. Lett.* **24** (2002) 247202.
12. Q.Y. Wen, H.W. Zhang, Y.Q. Song, Q.H. Yang, H. Zhu, and J.Q., Xiao, *J. Phys. Condens. Matter* **19** (2007) 246205.